Cosmic Ray Spallation in Radio-Quiet Active Galactic Nuclei: A Case Study of NGC 4051

T.J.Turner

Department of Physics, University of Maryland Baltimore County, Baltimore, MD 21250 and Astrophysics Science Division, NASA/GSFC, Greenbelt, MD 20771, U.S.A

and

L.Miller

Department of Physics, University of Oxford, Denys Wilkinson Building, Keble Road, Oxford OX1 3RH, U.K.

ABSTRACT

We investigate conditions for and consequences of spallation in radio-quiet Seyfert galaxies. The work is motivated by the recent discovery of significant line emission at 5.44 keV in *Suzaku* data from NGC 4051. The energy of the new line suggests an identification as Cr I Kα emission, however the line is much stronger than would be expected from material with cosmic abundances, leading to a suggestion of enhancement owing to nuclear spallation of Fe by low energy cosmic rays from the active nucleus. We find that the highest abundance enhancements are likely to take place in gas out of the plane of the accretion disk and that timescales for spallation could be as short as a few years. The suggestion of a strong nuclear flux of cosmic rays in a radio-quiet Seyfert galaxy is of particular interest in light of the recent suggestion from *Pierre Auger Observatory* data that ultra-high-energy cosmic rays may originate in such sources.

Subject headings: galaxies: active - galaxies: individual: NGC 4051 - galaxies: Seyfert - X-rays: galaxies

1. Introduction

Recent X-ray data from *XMM-Newton*, *Chandra* and *Suzaku* has led to the discovery of narrow line emission in the 5 - 6 keV regime in several local Seyfert galaxies (e.g. Turner et al. 2002; Yaqoob et al. 2003). One popular interpretation of the lines has been as emission from so-called 'hotspots' on the accretion disk, i.e. enhanced emission related to events such as magnetic reconnections on the disk surface. The observed line profile is modified by Doppler and gravitational effects, depending on the inclination of the system to the observers line-of-sight and the radial location of the hotspot. A hotspot that co-rotates with the disk should show a periodic pattern of variations in line energy and strength with time (so long as the disk is not observed face-on). If the hotspot originates within $20r_g$ then general relativistic effects are predicted to be measurable using current X-ray data. Superposed on the periodic shifts, lines should show down-shifting in the peak energy of the line with time as the material spirals inward (Dovčiak et al. 2004). As disk hotspots are not expected to survive for more than a few orbits at small radii (Karas et al. 2001), observation of persistent lines apparently originating close to the event horizon would disfavor the disk hotspot model.

Alternatively, the shifted lines may arise in ejected blobs of gas (such as comprising a wind, e.g. Turner et al. 2004). In contrast to the hotspot model, lines originating from ejecta are expected to show non-periodic evolution with time as the gas moves outwards, and by tracing the line energy over time one can potentially constrain the acceleration or deceleration mechanism. In prin-

ciple then, one could distinguish disk hotspot and ejecta origins for line emission in the 5 - 6 keV band using time-resolved spectroscopy.

However, another model has been suggested, where observed lines may be identified as species of elements such as Cr and Mn that normally would be too weak to measure using current data, but whose strength has been enhanced owing to abundance changes in the emitting gas from spallation of Fe (e.g. Turner et al. 2002). The interaction of protons having kinetic energy $\gtrsim 30\,\mathrm{MeV}$ with matter can result in spallation of its heavy nuclei, creating enhanced abundances of elements lower in mass than the target nucleus. In the low energy regime the protons required for effective spallation need be only mildly relativistic, easily achievable in a number of astrophysical situations and therefore we might expect to observe spallation under a range of conditions. Indeed, spallation is known to significantly affect the abundance ratios in our own Galaxy (Reeves 1974; Lund 1989) where there is approximate energy equipartition between cosmic-ray protons and the magnetic and radiation fields. The most noticeable effects of spallation are that abundant nuclei such as C, N, O, Fe are broken down, increasing the fraction of lighter elements such that the emission or absorption profile of the gas is significantly different than expected for cosmic abundance material. However, the cross-sections are relatively low ($\sigma < 1000\,\mathrm{mb}$, Letaw et al. 1983; Silberberg et al. 1998; Tripathi et al. 1999, where 1000 mb is $10^{-24}\,\mathrm{cm}^2$), and significant abundance changes in a large mass of gas require either high proton flux and/or long timescales.

The conditions for and the consequences of cosmic ray production in AGN have been discussed in the past by several authors (Kazanas & Ellison 1986; Axford 1994; Cronin 2005; Nagano & Watson 2000). While the effects of spallation could be detectable in any waveband, the cross-section for spallation increases with atomic mass approximately as $A^{0.7}$ (Letaw et al. 1983); this, the high cosmic abundance of Fe and its observability over a wide range of ionization mean that signatures of spallation may be most easily detected in X-ray spectra of iron group elements. At low cosmic ray energies the primary products from the spallation of Fe, and their partial cross-sections for prompt production following collision with a 100 MeV proton are Mn (400 mb), Cr (352 mb), V (115 mb) and Ti (70 mb), where the cross-sections have been determined from code supplied by Silberberg et al. (1998). If we adjust the cross-sections to account for the decay of unstable isotopes, the effective cross-sections become Mn (247 mb), Cr (560 mb), V (163 mb) and Ti (136 mb), adopting the decay channels summarized in Table 1 of Skibo (1997) but neglecting decay of ^{53}Mn, whose half-life is 3.7×10^6 years. At X-ray energies, neutral species produce Kα emission at 5.9, 5.4, 4.9 and 4.5 keV respectively. Comparison of the partial cross-sections shows that the most notable abundance enhancements produced from spallation of Fe would be for Cr and Mn.

Spallation of Fe has been discussed previously to explain line emission at 5.6 and 6.1 keV as emission from ionized species of Cr and Mn in NGC 3516, although in that case the lines ratios did not agree well with those predicted by Skibo (1997) for spallation of disk gas (Turner et al. 2002). However, the simulations by Skibo (1997) were conservative regarding the level of abundance enhancement that could occur as a result of spallation in active nuclei. Skibo (1997) considered the requirements for abundance enhancement in the total mass of material surrounding an accreting black hole, requiring a high efficiency of proton creation to achieve high factors of enhancement for Cr and Mn abundance.

In recent years our understanding of the nuclear environs of Seyfert galaxies has evolved, with ever-increasing evidence for large columns of gas covering a wide range of ionization state shrouding the active nucleus and shaping the observed properties of AGN in the X-ray bandpass. In this paper we argue that, if the gas in the putative disk wind provides the target for proton spallation, rather than the body of accretion disk itself, then the predictions and consequences of the process could be very different from the calculations of Skibo (1997).

Recent *Suzaku* observations of NGC 4051 reveal a line at 5.44 keV that is steady in flux and energy over years (Turner et al. 2010) disfavoring disk hotspot and ejecta models for the line origin and motivating a reconsideration of the importance of spallation in AGN. Exploration of the conditions for and consequences of spallation in

AGN is the topic of this paper.

2. Summary of Observational Results from NGC 4051

Line emission has recently been found at 5.44 keV and 5.95 keV in 2005 and 2008 *Suzaku* observations of NGC 4051 (Turner et al. 2010). While potentially of interest with regard to an identification as Mn emission, the line at 5.95 keV line suffers a degree of contamination from the slightly broadened component of Fe Kα emission (Miller et al. 2009; Turner et al. 2010) and (to a lesser degree) the detector calibration source. Detailed analysis also showed the inferred significance of the line at 5.95 keV to be sensitive to the form of the continuum model. For these reasons we concentrate on the line at 5.44 keV and the inferred ratio of Fe/Cr in this work.

Principal components analysis can be used to decompose data into a mathematical solution showing the simplest constant and variable orthogonal vector set that can explain the observations. We applied this technique to the combined 2005 and 2008 data from *Suzaku* observations of NGC 4051. That analysis showed that a line at 5.44 keV and the neutral component of Fe Kα emission comprise part of a flat 'offset' spectral component that dominates the source spectrum at low flux levels (Miller et al. 2009).

The statistical case for a line at 5.44 keV is very strong in NGC 4051. The improvement to the spectral fit using a Gaussian line component to model the emission is $\Delta\chi^2 = 32$ corresponding to a detection at $> 99.9\%$ confidence; this was obtained using a local continuum parameterization and fitting the 2005 *Suzaku* data. Instead of using a local continuum parameterization one can derive a complex model for the full-band *Suzaku* and HETG data and again test for the presence of an additional line. We found that such an approach does not diminish the level of confidence at which this line is detected (Turner et al. 2010; Lobban et al. 2010). The fit yields a line energy (in the rest-frame of the host galaxy) $E = 5.44 \pm 0.03\,\mathrm{keV}$, line flux $n = 5.03^{+2.02}_{-2.01} \times 10^{-6}\,\mathrm{photons\,cm^{-2}s^{-1}}$ (1σ uncertainties are quoted throughout) and equivalent width (against the total continuum) 46 ± 16 eV for 2005 *Suzaku* data. In that fit the flux and equivalent width of the Fe Kα line component (observed at an energy $E = 6.410 \pm 0.015$ keV) were $n = 1.59 \pm 0.23 \times 10^{-5}\,\mathrm{photons\,cm^{-2}s^{-1}}$ and 195 ± 24 eV respectively. As the width of the 5.44 keV line was not determinable with existing data, it was held at $\sigma = 50$ eV as determined for Fe Kα (whose fitted width was $\sigma = 50^{+26}_{-33}$ eV) and justified based on the evidence from principal components analysis that the Fe Kα emission and the 5.44 keV emission have a common origin (Miller et al. 2009).

The *Suzaku* data were time-sliced and the line found to be detected in the six resulting time periods, conclusively demonstrating that it cannot be a statistical fluctuation in the mean spectrum. Further to this, the feature was determined to be present in all three operational CCDs (Turner et al. 2010).

Finally, we note that the background count rates contributes only 2.5% of the total count rate in the 5-7 keV band for the summed XIS spectral data during the 2005 observation when the source is relatively dim (and only 1.3% when the source is brighter, during 2008). There is no evidence for line emission at 5.44 keV in the background spectrum and the combined background spectra from 2005-2008 yielded an upper limit (at 90% confidence) on the flux of such a line to be $n < 4.14 \times 10^{-8}$ photons $\mathrm{cm^{-2}s^{-1}}$, i.e. $< 1\%$ of the detected line flux. The lack of a feature at comparable flux or equivalent width in the background data also rules out an origin of the 5.44 keV line as a detector feature.

The flux of the line at 5.44 keV was found to be consistent with a constant value across the time-sliced *Suzaku* data and in archived *XMM* data (Turner et al. 2010); thus the line shows up most prominently when the continuum level is low (Figure 1), supporting the result from principal components analysis. The line energy was also found to be consistent with a constant value and, as noted previously, these observations thus disfavor hotspot and ejecta models for the line.

In the rest-frame of the host galaxy the line may be identified as Kα emission from Cr I, in which case the observed line strength exceeds what might be expected from simple continuum illumination of material with cosmic abundance ratios. Strong Cr emission that appears linked to the Fe emission is naturally explained by the spallation process. The Anders & Grevesse (1989) abundance ratio is

100:1 between Fe:Cr; taking the fluorescence yields into account ($Y_{Fe} = 0.347$, $Y_{Cr} = 0.282$) we would expect line equivalent widths relative to the illuminating continuum to be observed in the approximate ratio 123:1 for Fe:Cr from photoionized gas; folding in the relative K-shell photoionization cross sections modifies the estimate to an approximate ratio 113:1 for Fe:Cr. In the absence of spallation, Cr Kα line emission should be immeasurably weak for most AGN observed with current X-ray instruments. Contrary to expectations, the observed equivalent width ratio in the low-state data for NGC 4051 is Fe/Cr= 4.24 ± 1.57, i.e. showing a significant deviation from the expected ratio with a factor of ~ 30 enhancement of Cr Kα emission relative to the line ratios expected for cosmic-abundance material. The degree of spallation indicated by the ratio Fe/Cr is much more pronounced than observed in the Milky Way, but more extreme spallation might be expected as very different conditions of cosmic ray flux and material exposure are thought likely to exist close to an active nucleus.

Fitting a simple Gaussian model to the Fe Kα emission in NGC 4051 gave constraints on the width of the line that suggested an origin for the emission lines at $r \simeq 0.065$ light days, or 2×10^{14} cm, with the 90% confidence range being $7 \times 10^{13} - 3 \times 10^{15}$ cm. The strength of the Fe line can be used to constrain the column density of the emitting region (Yaqoob et al. 2009) yielding $N_H \gtrsim 10^{24}\mathrm{cm}^{-2}$, and in the toroidal reprocessor model suggests a global covering factor $C_g \simeq 0.9$. Detailed spectroscopy of the 2008 *Chandra HETG* and 2005-2008 *Suzaku* data also show a large amount of absorbing gas along the line-of-sight, covering a range of column densities, ionization states and outflow velocities, supporting the high global covering derived from the line strength. Combining the observational constraints thus yielded a mass estimate $M \gtrsim 4 \times 10^{-4}\mathrm{M}_\odot$ for the line-emitting gas with 90% confidence range $5 \times 10^{-5} < M < 10^{-1}\,\mathrm{M}_\odot$ (Turner et al. 2010).

While the true total profile of Fe Kα may be more complex (Miller et al. 2009), the limit estimated from the simple Gaussian model fit to that line provides a useful mass estimate for examination of the general feasibility of processes in this case study.

3. Discussion

With the evidence for a strong anomalous line in NGC 4051 and the possible identification as Cr emission we explore the possible production of cosmic rays in radio-quiet AGN, the dependence of spallation on parameters of the system, and the consequences of the process with respect to current observational constraints.

3.1. Production of cosmic rays in AGN

The high luminosity observed in the X-ray bandpass for AGN is thought to be produced from ultraviolet photons originating in the inner accretion disk that are up-scattered to X-ray energies (e.g. Haardt & Maraschi 1991). The requirement for an up-scattering mechanism has led to the suggestion that a large flux of hot electrons exist in the vicinity of the inner accretion disk and consequently an accompanying flux of protons or heavier nuclei may be assumed to be present. For a steep power-law cosmic ray energy spectrum most spallation is caused by low energy protons, $E \lesssim 200\,\mathrm{MeV}$, which are only mildly relativistic ($\beta \lesssim 0.6$). Shock acceleration could produce such a population of protons, or mechanisms such as that of Blandford & Payne (1982), where plasma is accelerated by a magnetic field tied to the rotating accretion disk, which might then generate protons with those energies.

3.2. Calculation of abundance enhancements in the "thick target" limit

Crosas & Weisheit (1996) and Skibo (1997) have previously considered the possibility of spallation in AGN. Skibo (1997) considered specifically the spallation of Fe and its detectability in X-ray spectra, and in this section we follow closely his analysis. Skibo assumed the case where gas presents a thick target to protons: i.e. all the cosmic ray energy is absorbed or radiated and there is no diffusion of cosmic rays out of the region. At low proton energies their primary energy loss is through Coulomb collisions, with an energy decay length, expressed in units of column density, of approximately $\Lambda_C \simeq 10^{26}(E/\mathrm{GeV})^{1.455}\beta\,\mathrm{atoms\,cm}^{-2}$ (Skibo 1997) for protons of energy E and velocity relative to light β . Thus zones of gas that are opaque to X-ray photons, with $N_H > 10^{24}\,\mathrm{cm}^{-2}$, also efficiently ab-

sorb cosmic ray protons with $E \lesssim 100\,\mathrm{MeV}$, and for steep incident power-law cosmic ray spectra the "thick target" approximation is valid for column densities $N \gtrsim 10^{25}\,\mathrm{cm}^{-2}$ (the validity of the thick target approximation is discussed further in Section 3.3). Within the target, proton directions are efficiently made isotropic by Coulomb scattering and magnetic field deflections. The propagation of cosmic rays through such a target can be treated as a diffusion problem. Those cosmic rays then impact heavy nuclei, and the rate per target nucleus of spallation of species i into species j is

$$R_{ij} = 4\pi \int_0^\infty \sigma_{ij}(E) J(E) \mathrm{d}E, \qquad (1)$$

where $\sigma_{ij}(E)$ is the spallation partial cross-section for that reaction and $J(E)$ is the intensity in cosmic rays of kinetic energy E inside the diffusion region. In a thick target, $J(E)$ depends on the cosmic ray injection rate and inversely on the mass M of material through which the cosmic rays diffuse (Skibo 1997). The expectation number of spallation events per target nucleus, $\langle n_{ij} \rangle$, can then be written as

$$\langle n_{ij} \rangle = \frac{\Omega \tau L_{\mathrm{CR}}}{4\pi M} f(E_{\min}, E_{\max}, \Gamma, \sigma_{ij}, \Lambda_C, \Lambda_{\mathrm{inelastic}}) \qquad (2)$$

where τ is the length of time the material is exposed to cosmic rays, L_{CR} is the rate of AGN cosmic ray kinetic energy output and Ω is the solid angle covered by the target gas. f is a function integrated over cosmic ray energy whose kernel is a function of the input spectrum, here parameterized by a powerlaw in kinetic energy of index Γ with lower and upper cutoffs $E_{\min}, E_{\max}$, the spallation cross-section and the path lengths due to Coulomb and inelastic collisions, $\Lambda_{\mathrm{inelastic}}$. Skibo equated τ to the expected time for gas of mass M to be accreted into the black hole if the mean accretion rate is $\dot{M}$: $\tau \simeq M/\dot{M}$. He also wrote $L_{\mathrm{CR}} = \eta(r_{\mathrm{ISCO}})\dot{M}c^2$, where $\eta(r_{\mathrm{ISCO}})$ is the efficiency of conversion of gravitational energy into cosmic ray kinetic energy for accretion of matter into the innermost stable orbit, from which equation 2 may be written as

$$\langle n_{ij} \rangle = \frac{\Omega \eta(r_{\mathrm{ISCO}}) c^2}{4\pi} f(E_{\min}, E_{\max}, \Gamma, \sigma_{ij}, \Lambda_C, \Lambda_{\mathrm{inelastic}}) \qquad (3)$$

with the mass terms conveniently disappearing. After taking into account the network of reactions, Skibo found significant abundance enhancements were achieved for $\eta(r_{\mathrm{ISCO}}) \gtrsim 0.05$, assuming $\Omega = 4\pi$, and that enhancements of Cr comparable to those inferred in section 2 were found for $\eta(r_{\mathrm{ISCO}}) \simeq 0.1$. The Skibo (1997) assumptions result in a maximum predicted enhancement by a factor 15 for Cr Kα emission over that expected from unspallated solar abundance material, while depleting Fe by a factor 2. This enhancement corresponds to a predicted ratio for the line equivalent widths Fe/Cr=3, and the observed ratio is Fe/Cr=4.24 ± 1.57, consistent with this value.

To achieve consistency with the observed line ratio, the necessary value for η is uncomfortably large. However, the value of η is strongly dependent on the assumptions made and hence the timescale needed for significant spallation; thus we proceed to explore whether different assumptions may yield consistency with observed data *without* the need for very high efficiency or very long timescales for material bombardment.

3.3. Spallation in the "thin target" limit

A key assumption in the above is that all the cosmic ray energy is absorbed or radiated by a "thick target". However, the column densities required for this assumption to be valid are $N \gtrsim 10^{25}\,\mathrm{cm}^{-2}$ at low cosmic ray energies, so we should consider the effect of loss of cosmic rays from the bombarded region in targets of lower column density. In the thick target limit the rate of spallation per target nucleus increases with decreasing target column density (or mass), and hence for sufficiently low target mass the predicted spallation rate becomes unphysically large, owing to the neglect of the diffusion of cosmic rays out of the target. To solve for the spallation rate while accounting for diffusion losses would require knowledge of the target geometry and magnetic field strength and structure. However, we may *estimate* the column density at which the thick-target approximation breaks down by comparing the calculated collision rate per nucleus with that expected in the thin-target limit, where a nucleus is exposed to the incident flux of cosmic rays. Higher energy cosmic rays have lower Coulomb losses and diffuse more easily from the target, so we should consider the cross-section for collisions that convert Fe into Cr,

as we are interested in the validity of the approximation for the purposes of calculating Cr abundance enhancement. This approach to estimating the limits of validity of the thick target approximation is rather crude, and it neglects the possibility that a target with a very large internal energy in magnetic field could hold an enhanced cosmic ray density compared with its surroundings, but it does give an indication of the typical column density at which the thick target approximation is likely to break down.

Calculation of the partial cross-section for the spallation of Fe into Cr is described by Silberberg et al. (1998) and we use their code for that calculation. However, many of the products of an Fe-p collision are unstable nuclei, so here we follow Skibo (1997) and modify the cross-sections to allow for decay into other species (see also Section 1). A significant contribution to the net Cr production arises from decay of ^{50,52,54}Mn (we again neglect decay of ^{53}Mn owing to its long half-life). Including this cross-section in the integration kernel of equation 1, we find a spallation rate per Fe nucleus of $R_{\mathrm{Fe}\rightarrow\mathrm{Cr}} \simeq 2\times10^{-8}(10^{24}\mathrm{cm}^{-2}/N_{\mathrm{H}})\,\mathrm{s}^{-1}$, assuming a cosmic ray spectral index $\Gamma = 2.4$, a low energy cut-off 10 MeV and a cosmic ray luminosity of $10^{43}\,\mathrm{erg\,s}^{-1}$ irradiating a target shell at distance 2×10^{14} cm. We may compare this with the rate expected in the thin target limit, for which we find $R_{\mathrm{Fe}\rightarrow\mathrm{Cr}} \simeq 3.8\times10^{-8}\,\mathrm{s}^{-1}$, so we expect the transition from the thick to thin target regimes to be important at column densities $N_{\mathrm{H}} \simeq 10^{24}\,\mathrm{cm}^{-2}$, close to the value we infer for the line-emitting gas in NGC 4051. For lower column densities it is essential to use the more conservative thin target limit.

In terms of the efficiency of spallation, the thick target limit ensures a maximum number of spallations occur per cosmic ray, and hence the maximum amount of enhanced material is produced. The total amount of enhanced material would be less in the thin target case, but the number of spallations per target nucleus reaches a maximum, so the abundance change in the gas being bombarded could be more marked in a target of lower column density. We return to consideration of spallation efficiencies in section 3.5.

3.4. Efficiencies, masses and timescales

A crucial parameter in the calculation of abundance change is the timescale over which nuclei are exposed to cosmic rays. From the above we can see that a high value of $\langle n_{ij}\rangle$ may be obtained either by a high cosmic ray flux or by a long timescale, greater than $M/\dot{M}$. Assuming a bolometric luminosity $L_{bol} = 10^{43}\mathrm{erg\,s}^{-1}$ (Vasudevan & Fabian 2009, corrected to the Tully-Fisher distance 15.2 Mpc, Russell 2004) and accretion bolometric radiative efficiency $\eta^{\mathrm{BOL}} = 0.05$ we deduce a mass accretion rate $\dot{M} \simeq 0.0035\,\mathrm{M}_{\odot}\mathrm{year}^{-1}$. The mass of gas bombarded by the cosmic rays is model-dependent, as we discuss below, but for a generic mass of $M \sim 0.01\,\mathrm{M}_{\odot}$ the accretion timescale $M/\dot{M}$ is only about 3 years. This timescale is much less than the current growth timescale of the black hole, $\tau_{BH} \simeq M_{BH}/\dot{M} \simeq 5\times10^{8}$ years for black hole mass $M_{BH} = 1.7\times10^{6}M_{\odot}$ (Denney et al. 2009) and leaves open the possibility that gas could achieve significant enhancements in abundance of Cr with a low cosmic ray luminosity, if it can survive near the black hole without being either accreted or blown out.

3.5. Location of the enhanced gas

Arguably the first location to consider for the target gas is the accretion disk. However, simple models of spallation within the disk both require the spallation timescale to be sufficiently long to generate the inferred abundance changes, $\tau \simeq M_{\mathrm{disk}}/\dot{M}$, and predominantly generate enhanced abundances only in the inner regions of the disk (see Appendix). Spallation may well occur within the accretion disk, but it seems unlikely that the efficiency would be high enough to achieve the abundance changes that we observe, and we would require a mechanism that transports enhanced material from near the ISCO to larger radii for consistency with the line widths that we observe. While transportation of the spallated gas is possible via outflow mechanisms such as a disk wind, the spallated gas detected in NGC 4051 yields a limit on the outflow bulk velocity $v < 1200$ km s^{-1}. It is difficult to determine from X-ray spectroscopy whether the component of outflowing gas traced by He-like and H-like Fe absorption lines has been modified by spallation, as Cr would

be highly ionized in such a zone and would provide little X-ray opacity.

A more attractive possibility is that the target gas is not part of the accretion disk itself, but rather is material lying out of the plane of the disk, perhaps even in or near the broad line region. In this case a relatively small mass of gas could intercept a large fraction of the cosmic rays emitted from the AGN, leading to much higher spallation rates than would be inferred for spallation within the accretion disk. Detailed timing analysis of the NGC 4051 data shows frequency-dependent time lags between the hard and soft X-ray photons of up to 970s. These may be explained by the effect of reverberation in the hard X-ray band as continuum photons are reflected from a thick shell of circumnuclear material extending to $\sim 1.5 \times 10^{14}$ cm from the black hole, having global covering factor $\gtrsim 0.44$ (Miller et al. 2009). This shell could comprise at least some fraction of the target gas.

To estimate the expected spallation timescale in the thick target approximation, we should assume a high column density, $N \gtrsim 10^{25}\,\mathrm{cm}^{-2}$, and equivalently a relatively high mass of target gas, $M_{\mathrm{gas}} \gtrsim 4 \times 10^{-4}\,\mathrm{M}_{\odot}$, for the nominal radius of $2 \times 10^{14}\,\mathrm{cm}$ and high filling factor (section 2; recall that in the thick target approximation, the abundance enhancement for a given cosmic ray exposure time decreases with M). Comparing with the Skibo (1997) calculation, the exposure to cosmic rays would need to last $\tau \gtrsim M_{\mathrm{gas}}/\dot{M} \gtrsim 4 \times 10^{-4}/0.0035 \simeq 0.11$ years for $\eta = 0.1$ (equivalent to a cosmic ray luminosity $2 \times 10^{43}\,\mathrm{erg\,s}^{-1}$). If we adopt a less extreme value for the efficiency of cosmic ray production, we would still only require the gas to be exposed to cosmic rays for a time $\tau \gtrsim 1.1/\eta$ years. The reason for the dramatic change in timescale, and the less restrictive requirement for the efficiency η, compared with the accretion disk case or with the Skibo (1997) analysis, is the higher rate of cosmic ray bombardment per Fe atom in the target gas. A small fraction of the gas in the accreting system receives a disproportionately high fraction of the cosmic rays. This of course is quite natural in the standard accretion disk picture, where most of the mass is in the disk but where additional traces of material are exposed to the central source over the remainder of the 4π sr.

For lower column densities and target masses, the timescale needed for significant spallation is expected to asymptotically approach the inverse spallation rate $\tau \rightarrow 1/\dot{R}$ for exposure to the incident cosmic ray flux (section 3.3), which for Fe with the assumed cosmic ray spectrum, luminosity $10^{43}\,\mathrm{erg\,s}^{-1}$ and radius $2 \times 10^{14}\,\mathrm{cm}$ is $\tau \gtrsim 0.9$ years. This estimate for low column densities yields a similar value to the thick-target calculation, albeit not one that takes into account the network of reactions as in the calculation of Skibo (1997).

If we knew the detailed geometry and magnetic field structure of the target we should solve the diffusion-loss equation for some assumed system mass and diffusion loss coefficient, but in either the thin- or thick-target case the required timescale is only of order years, and over the lifetime of the black hole growth, a substantial total amount of material could be processed through the cosmic ray region: at any one instant of time we only need to be observing a small mass of spallation-enhanced gas which could have been substantially enhanced in its Cr abundance. This scenario is an effective way of explaining the apparent abundance enhancements that we see without requiring extreme conditions of cosmic ray production.

3.6. Gamma-ray and radio emission

Interactions of cosmic rays with the accreting gas are expected to produce secondary γ-ray emission (Dermer 1986) and Skibo (1997, equations 11-12) estimated the γ-ray flux above 100 MeV for Seyfert galaxies if spallation is occurring. We have recalculated the expected γ-ray flux specifically for NGC 4051 following Skibo (1997). The estimate considers only production of γ-rays following neutral pion creation, as calculated for the Milky Way by Dermer (1986), whose code we use for the calculation, modified to incorporate equation 4 of Skibo (1997). The calculation assumes the "thick target" case where all protons are absorbed, and hence this provides a maximum γ-ray luminosity for a given output AGN proton luminosity. Assuming that $L_{\mathrm{CR}} = L_{bol}$, the predicted γ-ray flux is $F(>100\,\mathrm{MeV}) \simeq 3.3 \times 10^{-8} (\Omega/4\pi) \mathrm{photons\,s}^{-1}\,\mathrm{cm}^{-2}$ for proton spectral index $\alpha = 2.4$ and proton low-energy cut-off 10 MeV. About 0.8 percent of the input cosmic ray energy is radiated as γ-rays. For this proton input spectrum, the γ-ray spectrum is harder, with an approximately power-law form with photon in-

dex 2.1 in the range 100 MeV< $E_\gamma < 100$ GeV. Abdo (2009) discuss the detection limit of the *Fermi* Large Area Telescope and for $\Omega \sim 0.9$ the predicted flux of NGC 4051 falls just below the 10σ detection limit from the 3-month sky survey data $\sim 3.5 \times 10^{-8}$photons s^{-1} cm^{-2} for a source of this spectrum and Galactic coordinates (Abdo 2009). A "thinner" target in which protons escape the AGN, lower global covering factors, lower cosmic ray luminosities achieved through longer spallation timescales or the possibility of intermittent cosmic ray output all weaken the possible constraints available from measurements of γ-ray flux.

Radio synchrotron emission might also be expected, partly as a result of secondary electron creation but more significantly through primary cosmic ray electrons generated as part of the process that accelerates the protons. Any estimate of the synchrotron emission is extremely uncertain, as we don't know the efficiency of electron acceleration compared with proton acceleration, we don't know the magnetic field strength and the electrons themselves are expected to suffer significant ionization losses propagating through the material as well as adiabatic and radiative losses through bremsstrahlung, synchrotron and inverse Compton scattering. Furthermore, any compact synchrotron-emitting region would be self-absorbed, significantly reducing the detectability of any synchrotron emission. We do not here solve the diffusion-loss equation for electrons, but we can already place a stringent limit from simple estimates of the radiative losses. The ratio of synchrotron to inverse Compton losses is given approximately by the ratio of energy densities in magnetic fields, u_{mag}, and radiation, u_γ, so if these were the dominant energy loss mechanisms, we would expect an integrated synchrotron luminosity

$$L_{\rm sync} \simeq L_{\rm electron} \frac{u_{\rm mag}}{u_\gamma + u_{\rm mag}}$$

neglecting synchrotron self-absorption for the moment. If other mechanisms lead to comparable energy losses, the synchrotron luminosity would be lower. NGC 4051 has an steep spectrum radio core with flux density 3.2 mJy at 5 GHz when measured at resolution 1.1 arcsec (Ho & Ulvestad 2001), corresponding to a spatial resolution 80 pc. The core has been claimed to be marginally detected at EVN resolution (Giroletti & Panessa 2009). The core radio luminosity of NGC 4051 integrated up to 100 GHz is approximately 3×10^{37} erg s^{-1}, so we can place an approximate upper limit on the magnetic field strength if we require $L_{\rm sync}$ to be less than this value. For $L_{\rm electron} \simeq L_{\rm bol} \simeq 10^{43}$ erg s^{-1} and an energy density in radiation at $r = 2 \times 10^{14}$ cm of $u \simeq 700$ erg cm^{-3} we find $u_{\rm mag} < 0.002$ erg cm^{-3}, corresponding to a magnetic flux density $B < 0.2$ Gauss. In the synchrotron-optically-thin regime a discrepant radio flux could only be produced if B were higher than this value, but then any mJy synchrotron source with magnetic field higher than this value would be strongly self-absorbed at GHz frequencies on these angular scales. So even without consideration of the other energy loss mechanisms, we conclude that no significant excess of radio emission would be expected from the region. If some fraction of relativistic electrons escape to larger radii where inverse Compton losses are less severe and where the synchrotron surface brightness limit is not so restrictive, detectable radio emission could be produced, but without a detailed model for the electron energy losses and electron transport to larger radii, we cannot estimate its possible contribution to the observed radio emission.

3.7. Energy and momentum transfer

At low cosmic ray energies $\lesssim 1$ GeV, the cosmic ray energy is absorbed by either Coulomb interactions or inelastic scattering and spallation, and ultimately that energy ends up as either heat or kinetic energy (see also Crosas & Weisheit 1996). For a "thin" target the heating may be relatively low, but for a thick target we can estimate the energy density in the diffusing cosmic rays by evaluating the cosmic ray intensity $J(E)$ from equation 4 of Skibo (1997). Assuming $L_{\rm CR} = 10^{43}$ erg s^{-1} we estimate an energy density $u_{\rm CR} \simeq 240/N_{25}$ erg cm^{-3}, where N_{25} is the column density in units of 10^{25}cm^{-2}, assuming a powerlaw cosmic ray spectrum with index 2.4 above 10 MeV and a source-gas distance of 2×10^{14} cm. The expression is invalid for $N_{25} < 1$ as the gas would no longer satisfy the "thick target" assumption. For $N_{25} = 1$ the energy density is equivalent to the thermal pressure in gas of temperature 10^6 K with density 10^{12} cm^{-3}, so in sharing their energy with

the absorbing gas, the cosmic rays make a significant contribution to the thermal history of a thick target. The momentum transfer is similarly significant: in an equivalent of the "Eddington luminosity" calculation, for $L_{\rm CR} = 10^{43}\,{\rm erg\,s^{-1}}$ and column density $N = 10^{26}\,{\rm cm^{-2}}$ the rate of cosmic ray momentum transfer is 0.4 of the Eddington rate. These high values of energy and momentum deposition do not apply in the "thin target" regime, but if there were significant column densities of material intercepting the cosmic rays, they would be expected to experience significant heating and radial forces, as suggested by Sironi & Socrates (2009).

3.8. On the origin of UHECRs

The astrophysical origin of cosmic rays is a topic of great interest. Cosmic rays up to energies of 10^{15} eV appear to originate from supernova remnants, those in the range $10^{15} < E < 10^{18}$ eV also appear to have a Galactic origin, however, the source of ultra-high energy cosmic rays (UHECR) $E > 10^{18}$ eV is not yet accounted for. The extreme conditions in the nuclei of active galaxies offer an appealing possibility for production of UHECRs but cosmic rays have not yet been directly established as originating from active nuclei. While the cosmic rays required for spallation are of low energy, $\lesssim 1\,{\rm GeV}$, the mechanisms thought to be in play in AGN may also produce UHECRs.

To date, radio loud AGN have been the focus of studies of cosmic-ray production in AGN because radio jets have been widely thought to provide a suitable site for particle acceleration. However, even the jets of radio-loud AGN have fine-tuned requirements for successful particle acceleration: Farrar & Gruzinov (2009) argue that shock acceleration in a relativistic jet is constrained by the need to have a sufficiently strong magnetic field for acceleration of particles to energies above 10^{18} eV, while staying within a range that avoids over-production of synchrotron radiation and excessive photo-pion energy losses in the AGN.

It had been thought that UHECRs could not be produced in the nuclear regions of radio-quiet AGN because of the small size of the acceleration region and the energy losses (e.g. Norman et al. 1995). However new work by Pe'er et al. (2009) has argued that nearby radio-quiet AGN could indeed be the source of UHECRs. Pe'er et al. (2009) consider particle acceleration in the parsec-scale weak jets that are known to exist in many local radio-quiet AGN including NGC 4051 (Giroletti & Panessa 2009). However, recent *AUGER* results have suggested that UHECRs may be dominated by heavy nuclei (Unger et al. 2007; Bellido et al. 2009), and in this case the constraints on jet luminosity are reduced. Pe'er et al. (2009) calculate conditions for a bolometric luminosity $10^{43}{\rm erg\,s^{-1}}$, applicable to NGC 4051, and find that the nucleus can survive photo-disintegration if the acceleration occurs on a parsec scale, concluding that radio-quiet AGN are viable sources of UHECRs.

The relationship between the observed photon flux and currently observed cosmic ray flux from a particular galaxy is unclear, owing to the significant time delay that must exist for the arrival at Earth of cosmic rays compared with X-ray photons (of order 10^5 years; Moskalenko et al. 2009). However one can attempt to conduct a statistical survey of the coincidence of UHECR occurrence and the positions of AGN. Intriguingly, Zaw et al. (2009) have discovered a significant angular correlation between low luminosity AGN and high-energy cosmic rays in data from the Pierre Auger Observatory. The correlation is too strong to be simply explained by AGN tracing the large-scale distribution of matter, indicating that a significant fraction of UHECRs are produced in AGN (Farrar et al. 2009).

Moskalenko et al. (2009) suggest that as the UHECR candidate AGN have no special characteristics to set them apart from the AGN population (i.e. they are not the radio-loud sources) then the apparent correlation of low luminosity AGN with UHECRs must be a chance occurrence. Zaw et al. (2009) note that the candidate AGN may not appear 'special' at any given time if cosmic ray acceleration occurs via a sporadic event such as tidal disruption, which may inject $> 10^{52}$ ergs into the nuclear environs (Farrar & Gruzinov 2009) and yet not be occurring at the time of observation of the candidate AGN. Tidal disruption events should only occur every $10^4 - 10^5$ years (Magorrian & Tremaine 1999) in a given AGN and the duration of the event itself would likely be very brief, of the order of tens of rotations at the innermost stable orbit, i.e. hundreds to thousands of seconds in the case of NGC 4051.

However, current data cannot rule out the possibility that modest luminosity, radio quiet AGN commonly and persistently produce cosmic rays in their nuclear environs. As the typical number of UHECR detected is only ~ 1 per AGN, Poisson sampling guarantees that not all AGN will have associated UHECR in the Pierre Auger Observatory data. If UHECR production is linked to production of low energy cosmic rays in AGN, signatures of spallation may be better indicators of cosmic ray acceleration rather than large-scale radio jets, and invoking a sporadic event for cosmic-ray acceleration appears unnecessary. If spallation is occurring in NGC 4051, then this provides important observational evidence for the existence of a significant flux of low energy cosmic-rays in radio-quiet active galactic nuclei, and by extension is supportive of the production of UHECRs from the same sources.

4. Conclusions

Significant line emission at 5.44 keV in NGC 4051 may be interpreted as evidence for spallation at work in the nucleus of a radio-quiet active galaxy. Examining conditions for and consequences of spallation in circumnuclear material we find the highest abundance enhancements are likely to take place in target gas away from the plane of the accretion disk with timescales for spallation that could be as short as a few years if the cosmic ray output is comparable to the bolometric output of the active galaxy. Spallation timescales would be proportionally longer for lower cosmic ray luminosity, but even so could still be orders of magnitude shorter than the accretion timescale onto the black hole. Feedback of material from the active nucleus to the host galaxy may result in enhanced abundance ratios at larger radii than probed with these X-ray observations.

As the acceleration processes required to produce the protons necessary for spallation likely produces a broad spectrum of energetic particles, the results are also interesting in the context of our broader understanding of the origin of cosmic rays. The evidence for spallation in this radio-quiet active galaxy may support the discovery from the *Pierre Auger Observatory* data that the origin of ultra-high-energy cosmic rays may be the nuclei of radio-quiet AGN rather than luminous radio-loud AGN.

We are grateful to C. Dermer for supplying his code to calculate secondary γ-ray emission from neutral pion production, TJT acknowledges NASA grants NNX09AO92G and GO9-0123X. LM acknowledges STFC grant number PP/E001114/1.

A. Appendix material

A.1. Accretion disk spallation

We might suppose that material in the accretion disk is exposed to cosmic rays. However, in the simplest pictures, spallation would occur primarily close to the black hole and would be limited by the accretion timescale assumed by Skibo (1997), $\tau \simeq M/\dot{M}$. Consider accretion disk material being illuminated by cosmic rays from a source a height d above the disk on the rotation axis. An annulus on the disk containing mass $\mathrm{d}M$ and subtending a solid angle $\mathrm{d}\Omega$ at d, has a cosmic ray intensity

$$J \propto \frac{L}{4\pi} \frac{\mathrm{d}\Omega}{\mathrm{d}M}$$

if the cosmic rays are localized to that radius, as expected for the very high column density in the accretion disk. If mass flows through that annulus at a radially-invariant rate $\dot{M}$ the expectation value for the number of spallations per nucleus is

$$\mathrm{d}\langle n_{ij} \rangle \propto \frac{L}{4\pi} \frac{\mathrm{d}\Omega}{\dot{M}}$$

and so the total number of spallations per nucleus integrated from infinity to radius r is

$$\int_{\Omega}^{2\pi} \mathrm{d}n(\Omega) = \frac{L}{2\dot{M}} \frac{d}{\sqrt{d^2 + r^2}}.$$

Thus half the expected spallation events occur within a radius $r_{1/2} = \sqrt{3}d$. The total number of spallations is half the value calculated by Skibo (1997) owing to the global covering factor of the disk of 0.5, but the spallation timescale has the value he assumed.

We reach a similar conclusion if we suppose instead that cosmic ray sources, perhaps associated with shocks in the accretion disk, are embedded within the disk. We gain a factor 2 if the cosmic rays are now all intercepted by thick disk material. If the cosmic ray intensity as a function of radius is given by the gradient in potential energy, then for Keplerian orbits in a Newtonian potential ϕ we expect

$$J \propto \frac{\epsilon c^2}{2} \frac{\mathrm{d}\phi}{\mathrm{d}t},$$

where ϵ is the efficiency of converting gravitational potential energy into cosmic ray energy[1]. Note that the mass of an element of gas cancels as in Skibo 1997. The expected number of spallations per nucleus at radius r is

$$\langle n_{ij} \rangle = \eta(r) c^2 f(E_{\min}, E_{\max}, \Gamma, \sigma_{ij}, \Lambda_C, \Lambda_{\text{inelastic}}) \tag{A1}$$

which is the relation given by equation 3 for $r = r_{\text{ISCO}}$ and $\Omega = 4\pi$. The value of $\eta(r)$ should be calculated appropriately for some assumed spin of the black hole, but for any metric the spallation occurs predominantly close to the ISCO.

---

[1]The relationship between ϵ and $\eta(r)$ for accretion in to radius r is

$$\eta(r) = \frac{\epsilon}{2c^2} \int_r^{r=\infty} \mathrm{d}\phi = \frac{\epsilon G M_{BH}}{2rc^2}$$

assuming Keplerian orbits in Newtonian gravity and

$$\eta(r) = \epsilon \left[1 - \frac{(1 - 2GM_{BH}/rc^2)}{\sqrt{1 - 3GM_{BH}/rc^2}} \right]$$

for circular orbits in a Schwarzschild metric. Note that the energy released from accretion must be partitioned between all forms of energy output from the active nucleus: i.e. it is not possible to have a Schwarzschild black hole producing electromagnetic radiation and cosmic rays with $\eta(r_{\text{ISCO}}) = 0.057$ in *both* outputs simultaneously.

Thus in either case, we reach the follow conclusions: (i) the spallation timescale is about the same as the accretion timescale, $\tau \simeq M/\dot{M}$, so to achieve large abundance changes a high efficiency of cosmic ray production is needed, $\eta(r_{\rm ISCO}) \gtrsim 0.1$; (ii) spallation in the accretion disk would be expected to occur primarily in the inner regions unless the cosmic ray source is very extended and/or distant from the disk. Yet the Fe Kα line, which we suppose originates in the same enhanced gas, is narrow, with a likely location $r > 7 \times 10^{13}$cm (section 2). However, we don't necessarily observe the gas in the same location as where the spallation occurred: thus an accretion disk origin for the spallation would require gas that has been enhanced near the black hole to have been transported back out to the large radii where we observe it.

REFERENCES

Abdo, A. A. e. a. 2009, ApJ, 700, 597

Anders, E. & Grevesse, N. 1989, Geochim. Cosmochim. Acta, 53, 197

Axford, W. I. 1994, ApJS, 90, 937

Bellido, J. A. et al.. 2009, arXiv:0901.3389

Blandford, R. D. & Payne, D. G. 1982, MNRAS, 199, 883

Cronin, J. W. 2005, Nuclear Physics B Proceedings Supplements, 138, 465

Crosas, M. & Weisheit, J. 1996, ApJ, 465, 659

Denney, et.al. 2009, arXiv:0904.0251

Dermer, C. D. 1986, A&A, 157, 223

Dovčiak, M., Bianchi, S., Guainazzi, M., Karas, V., & Matt, G. 2004, MNRAS, 350, 745

Farrar, G. R. & Gruzinov, A. 2009, ApJ, 693, 329

Farrar, G. R., Zaw, I., & Berlind, A. A. 2009, arXiv: 0904.4277

Giroletti, M. & Panessa, F. 2009, ApJ, 706, L260

Haardt, F. & Maraschi, L. 1991, ApJ, 380, L51

Ho, L. C. & Ulvestad, J. S. 2001, ApJS, 133, 77

Karas, V., Martocchia, A., & Subr, L. 2001, PASJ, 53, 189

Kazanas, D. & Ellison, D. C. 1986, ApJ, 304, 178

Letaw, J. R., Silberberg, R., & Tsao, C. H. 1983, ApJS, 51, 271

Lobban, A., Reeves, J., Turner, T. J., Miller, L., Braito, V., Crenshaw, D., & Kraemer, S. 2010, in preparation

Lund, N. 1989, in American Institute of Physics Conference Series, Vol. 183, Cosmic Abundances of Matter, ed. C. J. Waddington, 111–123

Magorrian, J. & Tremaine, S. 1999, MNRAS, 309, 447

Miller, L., Turner, T. J., Reeves, J. N., Lobban, A., Kraemer, S. B., & Crenshaw, D. M. 2009, arXiv: 0912.0456

Moskalenko, I. V., Stawarz, L., Porter, T. A., & Cheung, C. C. 2009, ApJ, 693, 1261

Nagano, M. & Watson, A. A. 2000, Reviews of Modern Physics, 72, 689

Norman, C. A., Melrose, D. B., & Achterberg, A. 1995, ApJ, 454, 60

Pe'er, A., Murase, K., & Mészáros, P. 2009, arXiv:0911.1776

Reeves, R. 1974, ARA&A, 12, 437

Russell, D. G. 2004, ApJ, 607, 241

Silberberg, R., Tsao, C. H., & Barghouty, A. F. 1998, ApJ, 501, 911

Sironi, L. & Socrates, A. 2009, arXiv:0902.1181

Skibo, J. G. 1997, ApJ, 478, 522

Tripathi, R. K., Cucinotta, F. A., & Wilson, J. W. 1999, Nuclear Instruments and Methods in Physics Research B, 155, 349

Turner, T. J., Mushotzky, R. F., Yaqoob, T., George, I. M., Snowden, S. L., Netzer, H., Kraemer, S. B., Nandra, K., & Chelouche, D. 2002, ApJ, 574, L123

Turner, T. J., Kraemer, S. B., & Reeves, J. N. 2004, ApJ, 603, 62

Turner, T. J., Miller, L., Reeves, J. N., Lobban, A., Braito, V., Kraemer, S. B., & Crenshaw, D. M. 2010, ApJ, submitted

Unger, M., Engel, R., Schüssler, F., Ulrich, R., & Pierre AUGER Collaboration. 2007, Astronomische Nachrichten, 328, 614

Vasudevan, R. V. & Fabian, A. C. 2009, MNRAS, 392, 1124

Yaqoob, T., George, I. M., Kallman, T. R., Padmanabhan, U., Weaver, K. A., & Turner, T. J. 2003, ApJ, 596, 85

Yaqoob, T., Murphy, K. D., Miller, L., & Turner, T. J. 2009, MNRAS, 1508

Zaw, I., Farrar, G. R., & Greene, J. E. 2009, ApJ, 696, 1218

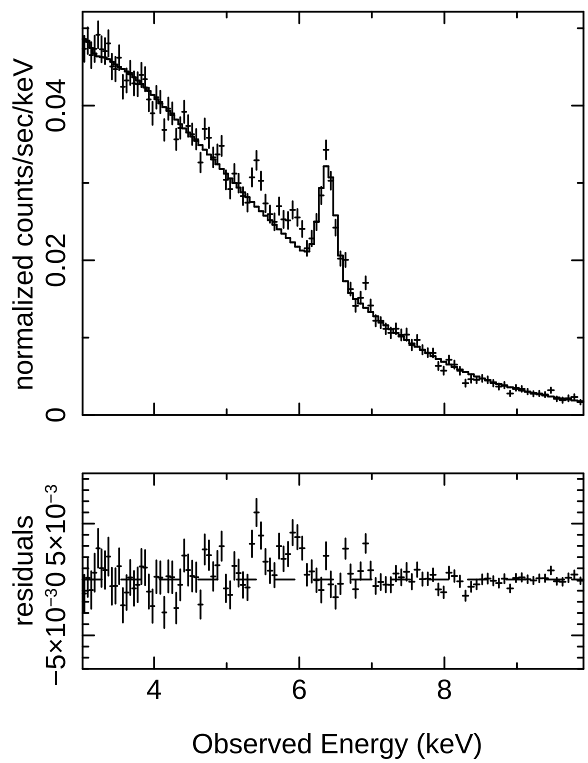

Fig. 1.— *Suzaku* XIS0 + 2 + 3 data and residuals from the mean 2005 spectrum, compared to an absorbed powerlaw plus Gaussian line at 6.4 keV, showing the residual excess counts at ∼ 5.44 and 5.95 keV

This 2-column preprint was prepared with the AAS LaTeX macros v5.0.